

Physical Drivers of the November 2023 Heatwave in Rio de Janeiro

Catherine C. Ivanovich¹, Adam H. Sobel^{1,2,3}, Radley M. Horton^{2,4}, Ana M. B. Nunes⁵, Rosmeri Porfirio da Rocha⁶, and Suzana J. Camargo^{2,4}

¹Department of Earth and Environmental Sciences, Columbia University, New York, NY, United States

²Lamont-Doherty Earth Observatory, Columbia University, Palisades, NY, United States

³Department of Applied Physics and Applied Mathematics, Columbia University, New York, NY, United States

⁴Columbia Climate School, Columbia University, New York, NY, United States

⁵Instituto de Geociências, Universidade Federal do Rio de Janeiro, Rio de Janeiro, RJ, Brazil

⁶Instituto de Astronomia, Geofísica e Ciências Atmosféricas, Universidade de São Paulo, São Paulo, SP, Brazil

Correspondence to: Catherine Ivanovich (cci2107@columbia.edu)

Abstract

As extreme heat has not historically been a major hazard for the city of Rio de Janeiro, the November 2023 Heatwave magnitude and timing were staggering. Here we conduct a case study of reanalysis data and high-resolution projections to explore the event drivers and characterize the evolving extreme heat risk in the city of Rio de Janeiro. We find that the heatwave was associated with atmospheric blocking, potentially linked to the 2023-24 El Niño event. Soil moisture declines increased surface sensible heat flux, and elevated sea surface temperatures reduced coastal cooling. The heatwave was preceded by weeks of suppressed precipitation and terminated by the onset of rain. We also find a significant historical increase in the frequency of high heat days throughout Brazil and a lengthening of the heat season in the city of Rio de Janeiro. The frequency of the city's austral spring heat extremes is expected to increase further in the future, highly dependent upon our future emissions pathway. These results emphasize the rapidly emerging risk for extreme heat in the city of Rio de Janeiro.

1 Introduction

In the spring of 2023, the city of Rio de Janeiro experienced a high impact heatwave that caught the world's attention. Media sources ranging from local reporting to international news companies centered stories on the event's record-breaking temperature magnitudes and unseasonal timing, arriving earlier in the warm season than typical heatwaves (Correio Braziliense, 2023; Hughs and Jeanet, 2023). The impacts of the extreme heat were widely publicized in part due to the tragic death of a concertgoer hospitalized during a Taylor Swift performance in Rio de Janeiro on November 17, with news articles reporting heat-induced cardiovascular distress as the cause of death (Nguyen, 2023). Sources also report that the stadium in which the concert took place experienced higher temperatures than those measured in the open air, as well as a lack of cooling equipment and insufficient water for attendees (Nguyen, 2023; Jornal Nacional, 2023). Such complexities highlight that extreme heat experienced by individuals on the ground can far exceed temperatures measured at local weather stations, depending on infrastructure and the capacity for cooling interventions (Wilby et al., 2021; Nahlik et al., 2017). However, the meteorological event itself is of course one of the preconditions for societal impacts. We therefore explore the physical mechanisms behind the heatwave as one key step towards improving preparation for the impact of future extreme heat events.

Deleted: .

Throughout Brazil, the highest temperatures occur climatologically in low latitude and low altitude regions in the interior of the country, such as the cities of Teresina (Piauí, in the Northeast region of Brazil) and Palmas (Tocantins, in the Central-West region of Brazil; Alvares et al., 2013), both of which are far from Rio de Janeiro. Extreme temperatures tend to be intensified by land-atmosphere interactions, as dry soils partition more energy into sensible heat (Geirinhas et al., 2018). These relationships between the atmosphere and land surface processes increase the likelihood of compound extreme heat and drought events and intensify impacts on agriculture (Cirino et al., 2015), worker productivity for outdoor laborers (Bitencourt et al., 2021), wildfire risk (Libonati et al., 2022), and direct impacts on human health (Zhao et al., 2019). As the frequency and intensity of extreme heat throughout Brazil has increased significantly in the past decades and is projected to continue in the future (Feron et al., 2019; Regoto et al., 2021; Bitencourt et al., 2020), the widespread socio-economic impacts of these events are likely to grow.

While Rio de Janeiro is the second most populous city in Brazil (Instituto Brasileiro de Geografia e Estatística 2022) and the third most populous city in South America (United Nations Department of Economic and Social Affairs Population Division 2022), few studies have focused on extreme heat in the city. On one hand, Rio de Janeiro has not historically been a major hotspot of extreme heat in Brazil and has experienced fewer heatwaves relative to other major cities in the country (Geirinhas et al., 2018). Further, the numerous microclimates within the city, influenced by its coastal setting and complex topography, complicate the study of local heatwave dynamics. Indeed, there is large spatial variability in temperature extremes across the Rio de Janeiro metropolitan area compared to other Brazilian cities (Alvares et al., 2013). However, impactful heatwaves in recent decades have increasingly drawn attention from public health officials and scientific communities alike. Recent literature has explored the dynamics and mortality impacts of extreme temperatures during heatwaves in 2010 (Geirinhas et al., 2019) and 2013/2014 (Geirinhas et al., 2022) and has begun to investigate compound heatwave and drought events throughout Southeast Brazil (Geirinhas et al., 2021). There is also building evidence that temperature extremes are increasing in intensity and frequency throughout Brazil, including the city of Rio de Janeiro (Regoto et al., 2021; Bitencourt et al., 2019). Climate variability also plays an important role in modulating temperatures over this area, including large scale modes of climate variability such as the El Niño-Southern Oscillation (Rehbein and Ambrizzi 2023; Cai et

al., 2020; Shimizu and Ambrizzi 2015), the Pacific Decadal Oscillation, and the Atlantic Multidecadal Oscillation (He et al., 2021). Should more intense, frequent, and unseasonably early extreme heat events take place in the future in the city of Rio de Janeiro, these heatwaves may have increased impacts on human health due to potential exceedance of unprecedented temperature thresholds and individuals' lack of preparation for these events. In a tropical city where baseline temperatures are already relatively high, small shifts in the temperature distribution can have large impacts on the frequency of extremes (Cheng et al., 2019), particularly at thresholds relevant to human health outcomes (Vecellio et al., 2022). These health risks are compounded by the humidity in Rio de Janeiro, a coastal city with ample moisture sources from the ocean and surrounding vegetation, priming the region for humid heat extremes which are physiologically more dangerous to human health than dry heat (Mora et al., 2017).

In this study, we explore the meteorological conditions that led to the extreme heat event in November 2023 in the city of Rio de Janeiro. We identify drivers of the exceptional magnitude and persistence of the extreme temperatures, as well as their early arrival in the calendar year. We compare these conditions to those associated with typical heatwaves in the region, and particularly events taking place in the spring season. We then consider how extreme spring temperature events have shifted throughout the historical period, and how we might expect them to change in the future with ongoing anthropogenic climate change.

2 Methods

2.1 Data

This analysis employs both station-based observations and reanalysis data. Initial analyses are conducted on subdaily station data from the city of Rio de Janeiro, accessed via the Met Office Hadley Center's HadISD station-based dataset (Dunn 2019) and the Rio Alert System produced by the Rio de Janeiro City Hall (Sistema Alerta Rio da Prefeitura do Rio de Janeiro 2024). Three airport weather stations are available from HadISD for the city of Rio de Janeiro, namely the Galeão/Antonio Carlos Jobim International Airport (located on the island Ilha do Governador within the Guanabara Bay), the Campo Délio Jardim De Mattos Airport (an Air Force base located in the city's North Zone), and the Santos Dumont Airport (a waterfront airport located near the city center). Six additional stations from the Rio Alert System dataset record measurements from the tops of various community and commercial buildings, including

109 hotels, schools, and warehouses. These stations are located in distinct areas of the city, whose
110 topographical and coastal complexities contribute to various microclimates. These stations thus
111 record distinct values, both instantaneously and on average (see Fig. S1), a challenge that has
112 been previously identified in the literature (Lyra et al., 2018; Dereczynski et al., 2013). We
113 therefore base the majority of our analysis on reanalysis data and compare the identified patterns
114 with station data when possible. This comparison is particularly important for extreme events, as
115 the magnitude of extreme heat has been shown to be biased in reanalysis products due to their
116 spatial and temporal smoothing of observations (Rogers et al., 2021; Raymond et al., 2020).
117 Further, the human experience of heat stress is inherently hyperlocal, meaning that the distinct
118 microclimates existing throughout the city can control heat stress exposure and the efficiency of
119 adaptation strategies. However, the present study is primarily concerned with the regional drivers
120 of the extreme event rather than its absolute magnitude. Reanalysis provides continuous spatial
121 coverage and a wide array of internally consistent meteorological variables, which warrants its
122 use for the application here.

123 Hourly meteorological data are retrieved from the fifth major global reanalysis of the
124 European Centre for Medium-Range Weather Forecasts (ERA5), including 2-meter temperature,
125 2-meter dewpoint temperature, volumetric soil water for layer 1 (0-7 cm, where the surface is at
126 0 cm), surface pressure, geopotential height at 500 hPa and 200 hPa, precipitation, evaporation,
127 2-meter horizontal winds, and vertical velocity at 500 hPa (Hersbach et al., 2020). From this
128 hourly data, daily maximum temperature, daily total precipitation, and daily means of all other
129 variables are calculated from 1979-2023. Daily mean sea surface temperature (SST) data from
130 1979-2023 is also retrieved from the NOAA 1/4° Daily Optimum Interpolation Sea Surface
131 Temperature (OISST) dataset (Huang et al., 2021).

132 We also explore the future evolution of temperature extremes over the city of Rio de
133 Janeiro using the NEXGDDP dataset (Thrasher et al., 2022). This data product is statistically
134 downscaled from the Coupled Model Intercomparison Project Phase 6 (CMIP6) models, with a
135 spatial resolution of 0.25 degrees and outputs variables on a daily temporal scale. We directly
136 retrieve daily maximum temperature data through the end of the century under the Shared
137 Socioeconomic Pathways (SSPs) SSP2-4.5 and SSP5-8.5 for the 23 models which output this
138 variable and pair of scenarios for each day in the calendar year through 2100.

Because of Rio de Janeiro's complex coastal and mountainous terrain, projections may not accurately capture fine scale differences in the city's climate. For example, recent literature has shown that the coastal cooling relative to inland areas experienced in regions such as the eastern United States may be underestimated by global climate models (Raymond and Mankin 2019). These biases are greatest in regions with large land-ocean surface temperature contrasts, however, and Rio de Janeiro's location in the tropics, as well as the fact that the extreme events analyzed in this study take place in the spring when this temperature gradient should be relatively small, may mute these biases compared to other regions and seasons. In order to address these potential sources of error, we generate a set of synthetic time series based on NEXGDDP projections which retain the seasonality and variability recorded in the historical reanalysis data from ERA5. We use a percentile matching technique in which we first bin all data for the grid cell which includes the city of Rio de Janeiro during a historical base period (1981-2013) into one-percentile bins for both the NEXGDDP and ERA5 datasets. We additionally bin all NEXGDDP data from this grid cell into one-percentile bins during one midcentury period (2041-2060) and one end-of-century period (2081-2100). We then calculate the temperature delta for each percentile bin between the base period and both the midcentury and the end-of-century periods in the NEXGDDP data. Finally, we add these percentile-specific change factors to every data point in each associated bin in the historical ERA5 base period.

2.2 Methodology

We first create time series for the historical day-of-year climatologies of variables in the city of Rio de Janeiro and compare them to the evolution throughout 2023. All anomalies are calculated relative to historical mean calendar date values (i.e., the daily maximum temperature anomaly on November 18, 2023 is calculated by subtracting the mean daily maximum temperatures on November 18 in all previous years in the historical record from the recorded absolute magnitude of the event). We also generate maps of concurrent meteorological variables relevant to the extreme heat event for the greater region outside of Rio de Janeiro. We compare these spatial patterns to those experienced during previous extreme heat events in Rio de Janeiro, calculated as 99th percentile daily maximum temperature days across all seasons for the grid cell which includes the Galeão International Airport weather station. We then select for events that occur in the September-November (SON) austral spring season.

We also quantify how extreme heat in the city of Rio de Janeiro is shifting using a variety of methods. We first calculate the trend in the frequency of extreme temperatures over the historical record in Brazil, defining these extreme temperatures using both absolute and relative thresholds. We select these thresholds as 30°C and the locally defined 90th percentile daily maximum temperature at each grid cell. These thresholds are chosen in order to investigate impactful temperature magnitudes while ensuring sufficient sample size for the trend analysis.

We also visualize the broadening of the extreme heat season, calculated based on the number of days between the start of the first heatwave and end of the last heatwave of the season. A heatwave is defined here as a three-day period with consecutive daily maximum temperatures above the 50th percentile of daily maximum temperatures across the two hottest months of the year in the city of Rio de Janeiro (January and February); this 50th percentile threshold is equal to about 31.4°C. This heat season definition is informed by a definition used by the United States Environmental Protection Agency (US EPA 2021), adapted to better reflect Rio de Janeiro's lower temporal variability in temperature due to its tropical location.

Finally, we calculate how spring temperature distributions have already changed in Rio de Janeiro by comparing early and late historical periods in ERA5 for the grid cell which includes the Galeão International Airport weather station. Distributions are calculated from annual spring maximum temperatures in the city of Rio de Janeiro and fit using GEV distributions, which have been shown to well capture extreme temperature distributions (Powis et al., 2023; Van Oldenborgh et al., 2022). For comparison, we also plot GEV distributions for early and late historical periods in the NEXGDDP model data before applying our bias-correction technique. The location parameter and spread of the model data distributions during these periods is much lower than that of ERA5 (Fig. S2), further motivating our use of synthetic time series to explore how these distributions may change in the future.

We then use the bias-corrected NEXGDDP data for the 23 models which report daily maximum temperature for each day in the calendar year under the aforementioned SSP2-4.5 and SSP5-8.5 scenarios during a midcentury and end-of-century time period. We additionally evaluate the impact of only using models which most accurately reproduce the historical observed daily maximum temperature record in the city of Rio de Janeiro. We calculate the Perkins skill score to evaluate the similarity between probability density functions of daily maximum temperature in the reanalysis dataset (ERA5) and each of the 23 global climate models

during the historical period. These skill scores are calculated as the cumulative minimum between the observed and modeled distributions of each binned value (Perkins et al., 2007). We finally select the 6 climate models which exhibit skill scores greater than 0.8, indicating that these models capture over 80% of the observed probability density functions. The result of this analysis is shown in Fig. S3, but the interpretation of the results as shown in the main text using all 23 models does not change.

3 Results

3.1 Rio de Janeiro's spring 2023 heatwave

The city of Rio de Janeiro experienced exceptionally high temperatures in both the austral winter and spring of 2023, peaking on November 18 (Fig. 1). This record-breaking event became the highest daily maximum temperature on record at the Galeão International Airport weather station, reaching 41.3°C. The extreme heat event was also notable for its accompanying high specific humidity, which rose alongside temperature in the days leading up to November 18 (Fig. 1b). The combination of elevated temperature and humidity rendered the event a humid heat extreme, as measured by wet bulb temperature, which peaked at 28.2°C on November 18 (Fig. 1c). The coincidence of extreme dry and wet bulb temperatures is typical for extreme heat events in Rio de Janeiro, where there is a statistically significant positive correlation between daily maximum temperature and daily mean specific humidity (Fig. S4). This relationship is facilitated by the city's abundant access to moisture from the coast and surrounding vegetation.

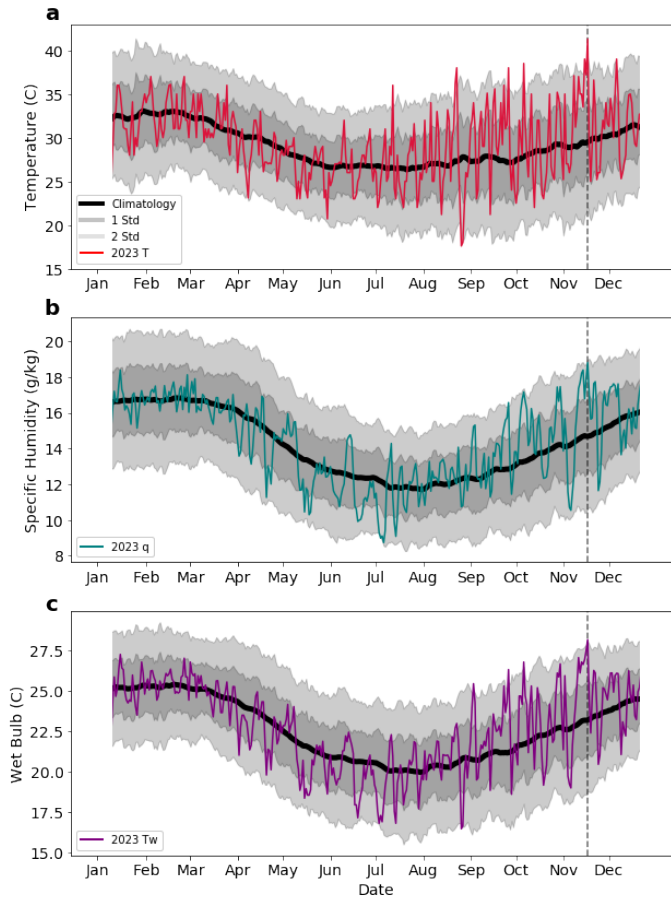


Figure 1: Historical climatology and 2023 recorded a) daily maximum temperature, b) daily mean specific humidity, and c) daily maximum wet bulb temperature in the city of Rio de Janeiro. Data from the Galeão International Airport weather station as reported by the HadISD dataset. Vertical dashed line identifies record-breaking temperature event on November 18, 2023.

Elevated temperatures occurred over an area greater than the city of Rio de Janeiro, but were spatially constrained by orography (Fig. 2). We explore the spatial patterns of the heatwave in data from the European Centre for Medium-Range Weather Forecasts (ERA5) reanalysis during the period of 1979-2023 (Hersbach et al., 2020). We see that hotspots in elevated

temperatures were located throughout the coastal region surrounding Rio de Janeiro, with sharp declines across the mountainous terrain moving inland. These positive coastal temperature anomalies coincide with northerly surface wind anomalies. ERA5 estimates the daily maximum temperature on November 18 in the grid cell containing the Galeão International Airport weather station as 40.6°C, within the range of temperatures recorded throughout weather stations in the city (Fig. 2c; Fig. S1). This extreme event was also remarkable in length as measured by ERA5, as daily maximum temperatures were above the locally defined 90th percentile for eight consecutive days, and above the 99th percentile for the final three days of this period (percentiles calculated from ERA5 across the period from 1979-2023). This multi-day interval of exceptional temperatures rendered it difficult for residents to find relief.

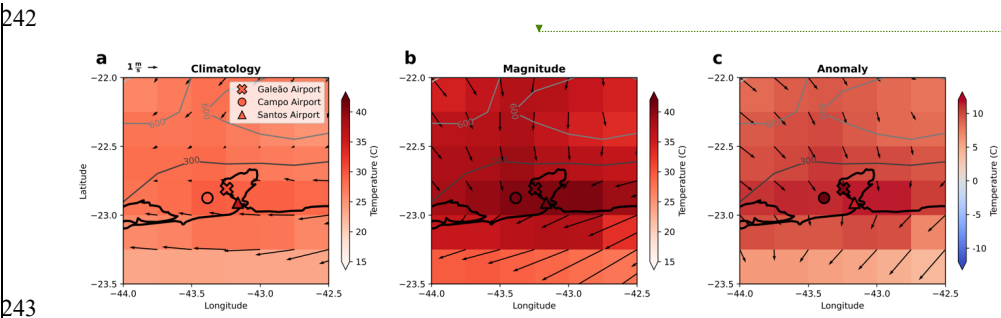
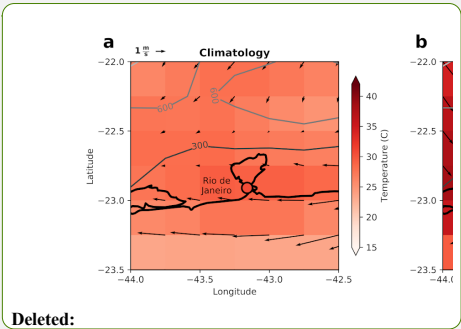


Figure 2: Spatial maps of daily maximum temperatures during the date of peak extreme heat intensity in the city of Rio de Janeiro using ERA5 data (shading) and three city weather stations with long-term temperature records (markers). Vectors represent surface winds; contours represent elevation in meters. A) Climatology during November 18 throughout the historical record. B) Magnitudes on November 18, 2023. C) Anomalies during November 18, 2023.

The maximum temperature during the event on November 18 coincided in time with other anomalous meteorological conditions (Fig. 3; for climatological values, see Fig. S5 in the Supplemental Materials). Positive geopotential height anomalies centered over Rio de Janeiro were consistent with an intensification of the South American Subtropical High, a semi-permanent anticyclonic circulation system off the Southeast coast of Brazil. The edge of this positive high pressure anomaly was collocated with the region of positive temperature anomalies that includes the city of Rio de Janeiro (Fig. 3b). Surface winds off the coast of Rio de Janeiro were anomalously northerly. Anomalously northerly flow in this mountainous area can



Deleted:
Deleted: the Galeão International Airport weather station ...
Deleted:

Moved (insertion) [2]
Deleted: Further,
Deleted: a

265 exacerbate high temperatures directly through downslope winds (Stefanello et al. 2022).
 266 Previous literature has also shown that anomalously northerly winds over the coast can increase
 267 local sea surface temperatures through reductions in wind-driven upwelling, reducing the
 268 capacity for coastal cooling (Castelao and Barth 2006; Palma and Matano 2009). Indeed, positive
 269 SST anomalies of up to 2°C occurred along Rio de Janeiro's coast on the day of the peak in air
 270 temperature (Fig. 3j). Anomalous winds over the interior of South America also enhanced the
 271 northerly South American Low Level Jet (Marengo et al., 2004; Montini et al., 2019). Positive
 272 specific humidity anomalies were present throughout Southeast and South Brazil (Fig. 3f),
 273 intersecting with an area of precipitation along the edge of the low pressure system to the south
 274 (Fig. 3g). The northern portion of the positive specific humidity anomaly was aligned with the
 275 positive geopotential height anomaly off the coast of Southeast Brazil. Widespread negative soil
 276 moisture anomalies occurred throughout most of Brazil, and the interior of South America more
 277 broadly, during this event (Fig. 3d). The large spatial coverage of these negative soil moisture
 278 anomalies was concurrent with Amazonian drought recorded during this time, inherited from the
 279 prior season (Espinoza et al., 2024). These spatial patterns are typical of extreme heat events
 280 during the spring season in the city of Rio de Janeiro, though the magnitudes of the anomalies in
 281 all of these variables are dramatically higher on November 18, 2023 than during other spring
 282 extreme heat events (Fig. 4). The most unique features of the November 18 event were the
 283 intensified northerly winds and the degree of inland penetration of positive specific humidity
 284 anomalies (Fig. 4e-f). Further, the positive local SST anomalies off the coast of Rio de Janeiro
 285 were particularly exceptional in intensity and spatial scale during this event, weakening the sea-
 286 air temperature contrast and sea-breeze (Fig. 4i-j). Outside of these specific distinctions, the
 287 event on November 18, 2023 was an intense example of a typical spring extreme heat event in
 288 the region.

Deleted: such

Moved (insertion) [1]

Deleted: Finally

Deleted: Ts

Moved up [2]: Further, anomalously northerly flow in this mountainous area can exacerbate high temperatures directly through downslope winds (Stefanello et al. 2022).

Moved up [1]: Finally, positive SSTs of up to 2°C occurred along Rio de Janeiro's coast.

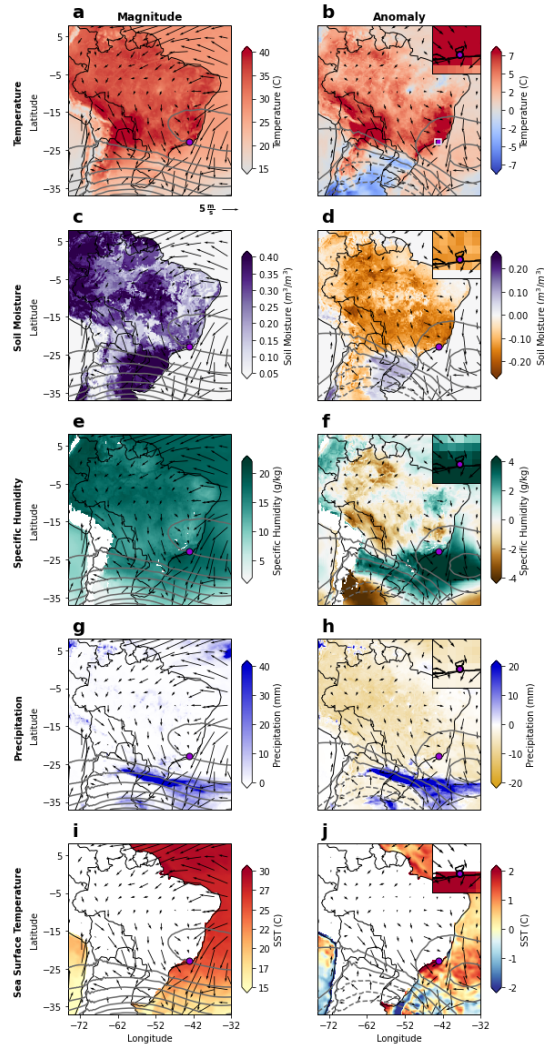


Figure 3: Magnitude (left) and anomalies (right) of daily maximum temperature, mean soil moisture, mean specific humidity, total precipitation, and mean SST on day of peak temperature in the city of Rio de Janeiro (November 18, 2023). Overlying wind vectors and 500 hPa geopotential height contours (50 m and 25 m contour levels for magnitude and anomaly plots, respectively). Anomalies calculated relative to historical calendar date mean values across the period from 1979-2023. Inset in the upper right corner of each anomaly plot zooms in on the white box surrounding the city of Rio de Janeiro (purple marker) in the top right subplot.

Deleted:

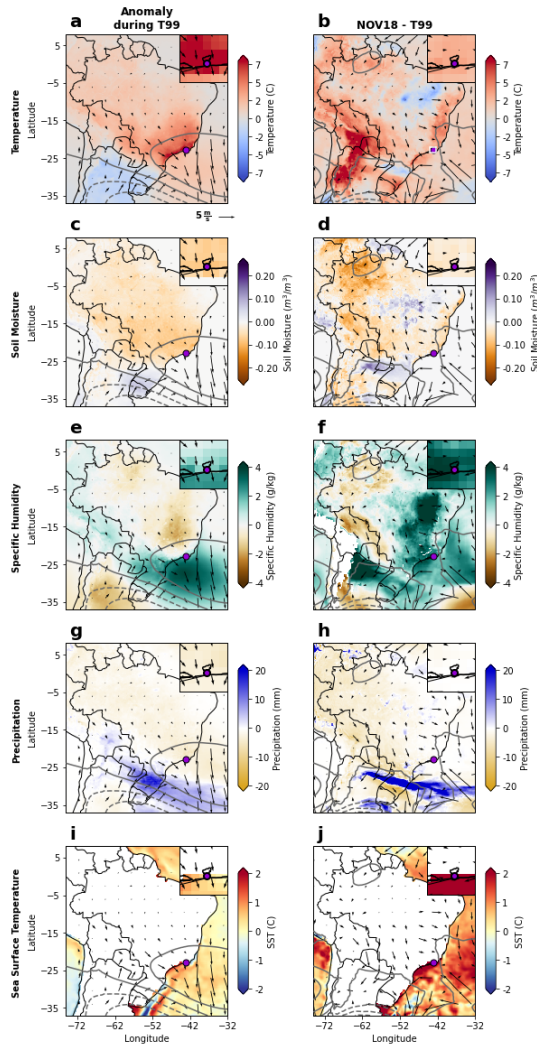


Figure 4: Anomalies in daily maximum temperature, mean soil moisture, mean specific humidity, total precipitation, and mean SST during 99th percentile extreme temperature days in the September-November (SON) season for the ERA5 grid cell which includes the Galeão International Airport weather station (left). Difference in conditions on November 18 compared to mean conditions during these 99th percentile extreme temperature days (right).

Deleted:

Formatted: Caption, Space After: 0 pt, Line spacing: single, Don't keep with next, Border: Top: (No border), Bottom: (No border), Left: (No border), Right: (No border), Between: (No border)

Deleted: ¶

316 The time evolution of the meteorological variables described above throughout the month
 317 of November 2023 uncovers the temporal development of the extreme heat event (Fig. 5). Rising
 318 temperatures throughout the weeks leading up to November 18 were preceded by elevated
 319 geopotential heights at 500 hPa and associated atmospheric subsidence. This was accompanied
 320 by a rapid decline in soil moisture which was likely facilitated by the increased solar insolation
 321 associated with the persistent high pressure system and resulting extremely low precipitation
 322 from November 2-November 18. Given that the rainy season in Southeast Brazil typically begins
 323 in late-October to mid-November (Coelho et al., 2021; Latinovic et al., 2018; Marengo et al.,
 324 2012; Liebmann and Mechoso 2011; Raia and Cavalcanti 2008), this period of consecutive dry
 325 days was unusual. Indeed, this period totals 17 days in a row with less than 5 mm of rain per day,
 326 and this only happened during the month of November in one other year in the historical record
 327 from ERA5 between 1979-2023 (2012). These changes in geopotential height, soil moisture, and
 328 suppressed precipitation preceded changes in other variables, evidenced by the grey lines in the
 329 background of each subplot. Wind direction was highly variable on a daily scale, but became
 330 increasingly northerly during this same period. These changes were accompanied by a gradual
 331 increase in SST off the coast of Rio de Janeiro, though delayed compared to that of the local air
 332 temperature. These changes in wind direction and SSTs are likely linked, as upwelling in this
 333 region can be significantly reduced through northerly wind anomalies, increasing coastal sea
 334 surface temperatures (Castelao and Barth 2006; Palma and Matano 2009). Secondary pathways
 335 to SST increases could include increased solar radiation to the ocean, added heat flux to the
 336 ocean, and a thinning of the oceanic mixed layer. These features are common around many
 337 coastlines during atmospheric heatwaves that are associated with warming coastal waters, though
 338 further research would be needed to quantify their relative importance during the November
 339 2023 heatwave in Rio de Janeiro. As air temperatures rose, specific humidity increased over the
 340 city. This was likely related to both local evaporation from the soil (co-occurring with declining
 341 soil moisture) and moisture advected from the anomalously warm coastal waters and surrounding
 342 vegetation. The circulation specifically on November 18 directed wind in the larger region
 343 surrounding Rio de Janeiro to intensify the South American Low Level Jet, which can
 344 additionally increase moisture transport from the Amazon Basin to Southeast Brazil (Marengo et
 345 al., 2004; Vera et al., 2006; Montini et al., 2019). However, convergence of the horizontal
 346 moisture flux at the level nearest the surface was only stronger than its climatological values in

Moved (insertion) [3]

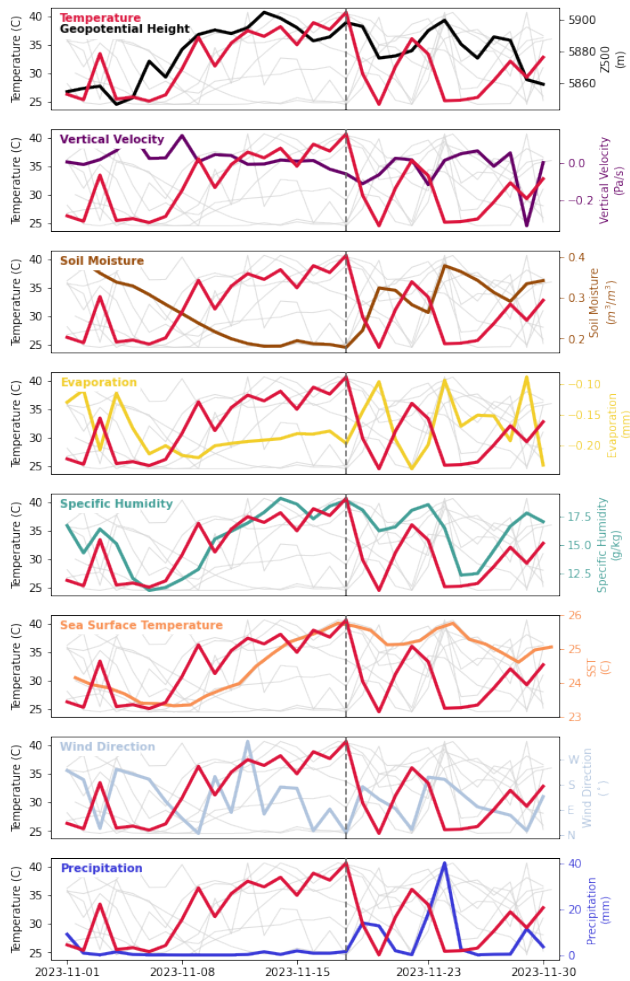
Deleted: There

Deleted: was also

Moved up [3]: Wind direction was highly variable on a daily scale, but became increasingly northerly during this same period. These

Deleted: coast

353 some grid cells within the northern and western areas of the city (Fig. S6). More generally,
354 specific humidity was also able to build without reaching saturation due to the increasing
355 temperatures (and the Clausius-Clapeyron relation). Finally, the heatwave was terminated when
356 a two-day precipitation event occurred from November 19- 20. This precipitation induced a
357 small decline in specific humidity and SST, as well as a rapid increase in soil moisture.
358



359

Figure 5: Evolution of meteorological conditions during the month of November 2023 in Rio de Janeiro. Grey lines in the background of each subplot show the evolution of all variables, with individual variables compared in colors to dry bulb temperature in red. Vertical dashed line identifies record-breaking temperature event on November 18, 2023. All variables are calculated for the grid cell which includes the Galeão International Airport weather station except SST, which is averaged over the box 21°S-24°S and 42°W-45°E.

The evolution of the 2023 heatwave as shown above is reminiscent of that during the 2010 heatwave analyzed by Geirinhas and coauthors (2019). Those authors explain that the extreme heat event in the summer of 2010 was initiated by a positive SST anomaly over the eastern Pacific that triggered a Rossby wave train that in turn intensified the South Atlantic Subtropical High. Modulation of this climatological high pressure system has been shown to be central to influencing weather in the city of Rio de Janeiro, and particularly temperatures there (Geirinhas et al., 2018). Here we also observe a positive SST anomaly over the equatorial Pacific throughout the month of November and a resulting anomalous wave pattern ending over the South Atlantic High that became increasingly organized and strengthened during the two weeks before November 18 (Fig. 6; see Fig. S7 in the Supplemental Materials for maps of the climatologies and absolute magnitudes of these variables). This mechanism is similar to how El Niño generally influences temperatures in Southeast Brazil on longer timescales (Cai et al., 2020), and we confirm that there is a positive correlation between the ENSO state as quantified by the Niño3.4 index and the frequency of high heat days in the city of Rio de Janeiro in the austral spring season (Fig. S8). Further, the mean spatial SST and Z200 patterns during the spring of typical El Niño years look very similar to those observed during November 2023, though the anomalies in both SST and geopotential height are much larger during November 2023 (Figure S9). 2023 was characterized by a transition from La Niña to El Niño, with the El Niño emerging in April-June 2023 and strengthening to a strong El Niño in the second half of 2023 (Becker et al., 2024). The SST anomalies associated with the El Niño could have been responsible for initiating the wave train which set off the geopotential height anomalies over Rio de Janeiro. More broadly, it has been suggested that multi-month elevations in temperature over Brazil throughout 2023 could be driven in part by El Niño (Pampuch et al. 2025). Further, the second half of 2023 was exceedingly warm globally (Cattiaux et al. 2024; Perkins-Kirkpatrick et al. 2024), due in large part to anthropogenic warming, indicating that climate variability and

393 climate change both likely preconditioned the November 2023 extreme heat event. We note that
394 similar wave trains driven by Pacific SST anomalies have been shown to influence weather in
395 Southeast Brazil even during neutral ENSO states (Seth et al., 2015). Additionally, the
396 instantaneous extreme temperature event and the preceding persistent dry conditions must also
397 be linked to the synoptic weather in the area. Decreases in soil moisture and horizontal moisture
398 fluxes by intensification of the South American Low Level Jet were central features of the
399 heatwave in 2010, as they were in November 2023. These overlaps in the apparent drivers of the
400 2010 and 2023 heatwaves underscore that while the 2023 spring event was unprecedented in its
401 magnitude and unusual in its spring timing, it was not unique in its overall dynamics.

Deleted:

Deleted: last year's

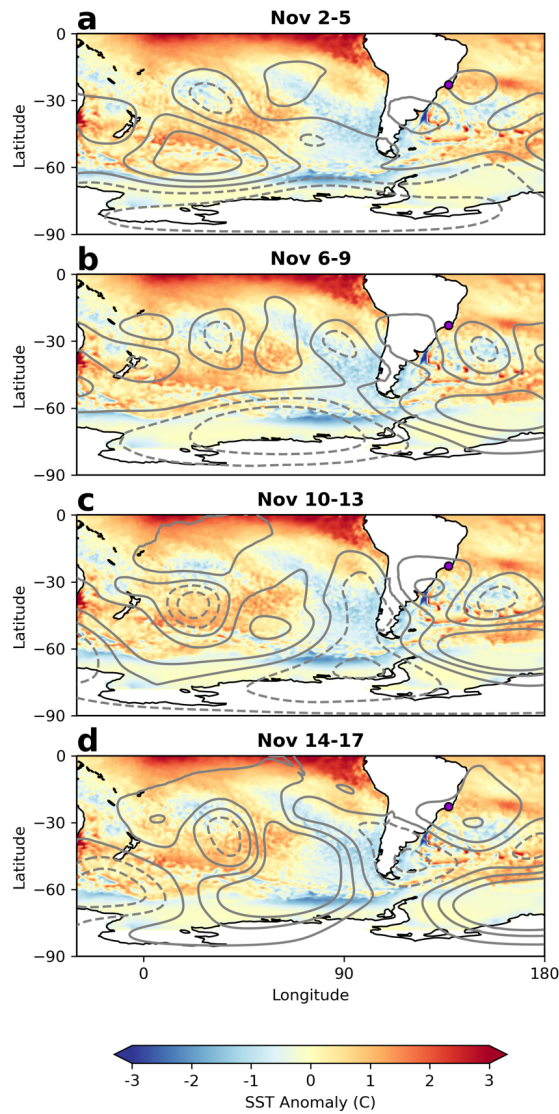


Figure 6: Evolution of the geopotential height at 200 hPa (contours) in the weeks of suppressed precipitation leading up to the extreme heat event on November 18 in the city of Rio de Janeiro. Geopotential height anomaly contour levels are at 100 m, with positive (negative) anomalies in solid (dashed) contours. Across all subplots, shading indicates November 2023 mean SST anomalies.

3.2 Historical and future changes in extreme heat

Extreme heat events have become more frequent in the city of Rio de Janeiro and the timing of these events has shifted earlier in the calendar year. There has been a significant increase in the number of days above 30°C each year over the past 44 years throughout almost all of South America (Fig. 7a). Further, the number of 90th percentile days locally defined at each grid cell has also increased significantly throughout most of the region (Fig. 7b). In the city of Rio de Janeiro specifically, the number of 30°C days per year during the austral spring is increasing at a rate of 0.27 days/year (Fig. 7c). Relative to 1979, the city now experiences almost 12 additional days per year above 30°C during the spring season alone. Overall, the extreme heat season in Rio de Janeiro is broadening. As measured by the number of days between the first and last heatwave day of the season (a period of three or more consecutive days with daily maximum temperatures above 31.4°C), the extreme heat season has lengthened from 156 days in the 1979-1980 season to 176 days in the 2022-2023 season (Fig. 8). The broadening of the heat season is due primarily to more early season heatwave days, while the end date of the heat season has not changed significantly.

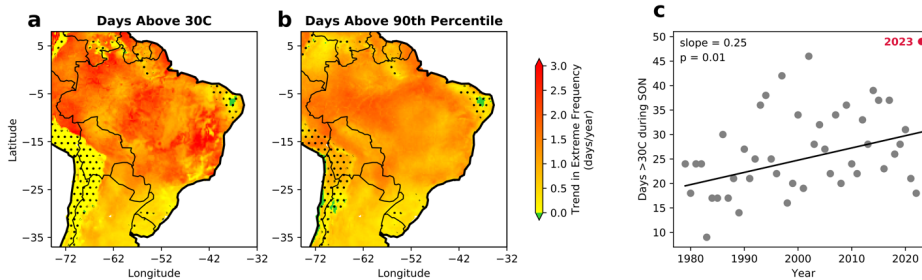


Figure 7: Historical trend from 1979-2023 in the number of days per year above a) 30°C and b) locally defined 90th percentile. Stippling shows areas which are not significant at a $p = 0.05$ level assessed using a Wald Test. c) Trend in number of days per year above 30°C taking place in the SON season in ERA5 for the grid cell which includes the Galeão International Airport weather station.

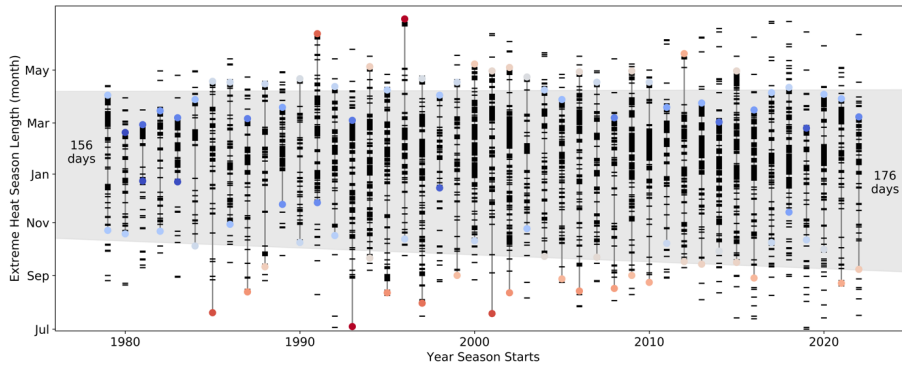


Figure 8: Shifting timing of the city of Rio de Janeiro extreme heat season. Horizontal axis indicates the year in which winter begins (“January” marking denotes the start of the following calendar year). Colored markers indicate the first and last days of the extreme heat season each year. Marker color indicates whether the start/end date is lengthening (red) or shortening (blue) the heat season compared to historical mean start/end dates. Dashes indicate individual additional days with daily maximum temperatures surpassing 31.4°C (no persistence required). Grey shading indicates area between trend lines in the shifting seasonality.

The distribution of maximum spring temperatures in the city of Rio de Janeiro has shifted higher over the last four decades and this pattern is projected to continue in the future. In order to evaluate whether the observed historical increase in extreme heat frequency identified in Figures 7 and 8 may continue in the future, we fit annual maximum spring temperatures from historical ERA5 reanalysis data and future projections from bias-corrected NASA Earth Exchange Global Daily Downscaled Projections (NEXGDDP) data (Thrasher et al., 2022, see Methods) to a Generalized Extreme Value (GEV) distribution. When comparing early and late historical periods from 1979-1988 and 2014-2023, respectively, the location parameter of the two GEV distributions has increased by 1.7°C (Fig. 9). The distribution of maximum austral spring temperatures in the city of Rio de Janeiro is also projected to continue shifting to higher values in the future, but the magnitude of this change is strongly dependent upon the future emissions pathway. The temperature distributions associated with mid-century periods (2041-2060) under SSP2-4.5 and SSP5-8.5 future scenarios are similar to that of the last 10 years of observational data, with shifts in the location parameters of 0.1°C and 0.9°C for the two emissions trajectories,

458 respectively. A larger change is projected by the end of the century (2081-2100) under each
459 emissions scenario. However, the end-of-century SSP5-8.5 scenario is distinctly separate from
460 the other distributions, with the distribution location parameter 2.8°C higher than during the last
461 10 years.

462 These changes to the distributions strongly influence the probability of an event with the
463 intensity of the maximum temperature recorded on November 18, 2023. The probability density
464 function fit to the projected annual maximum spring temperatures under each mid-century period
465 using a GEV distribution yields a return period for an extreme temperature event with the daily
466 maximum temperature at least 40.6°C in the city of Rio de Janeiro (analogous to the event on
467 November 18, 2023 as measured by ERA5) of 51 years under SSP2-4.5 and 33 years under
468 SSP5-8.5. By the end of the century under either emissions scenario, an event of this magnitude
469 becomes much more likely, with return periods of 19 years or just 4 years under SSP2-4.5 and
470 SSP5-8.5, respectively. [These return periods align well with estimates for station-level](#)
471 [projections from Collazo et al. 2025, which estimates a return period of 4 to 9 years for](#)
472 [heatwaves analogous to that of November 2023 for a future climate with global mean surface](#)
473 [temperatures 2°C warmer than preindustrial levels.](#) Recent literature has suggested that the
474 SSP5-8.5 scenario may not be realistic given our current socioeconomic, political, and physical
475 landscape (Hausfather and Peters 2020; Burgess et al., 2020; Ritchie and Dowlatabadi 2017).
476 However, these results indicate that an austral spring heatwave of the magnitude experienced in
477 the city of Rio de Janeiro on November 18 is projected to become much more frequent in the
478 future, even under the more stringent SSP2-4.5 emission pathway. [As temperatures rise and the](#)
479 [city of Rio de Janeiro maintains its ample moisture sources from the nearby ocean and](#)
480 [vegetation, we expect that humid heat extremes will also become more frequent and intense,](#)
481 [though at a slower rate than dry bulb temperature extremes as dictated by tropical atmospheric](#)
482 [dynamics \(Coffel et al. 2018; Zhang et al., 2021; Matthews et al., 2025\).](#) We must also note that
483 it is difficult to evaluate whether the models are missing emerging factors that could increase the
484 frequency and intensity of these extreme heat events – such as Amazonian deforestation or
485 declines in sea ice – reducing their ability to capture the possible future spring temperature
486 distributions in Rio de Janeiro.

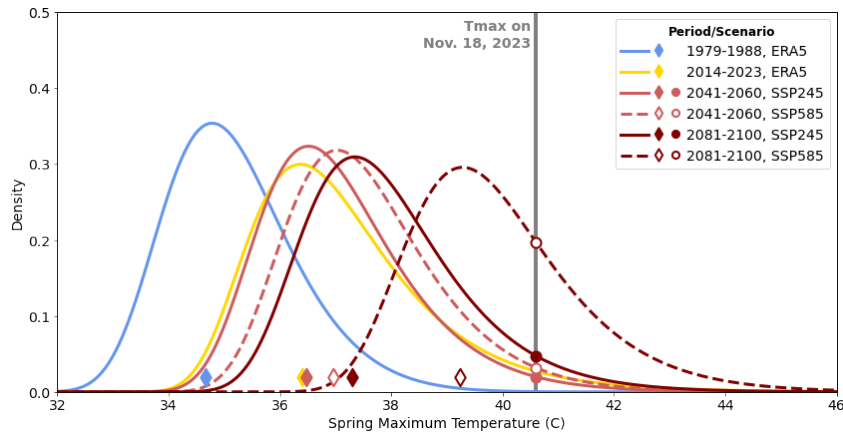


Figure 9: Generalized Extreme Value distributions for SON maximum temperatures during early and late historical periods (observed in ERA5), mid-century periods, and end-of-century periods under SSP2-4.5 and SSP5-8.5 (projections from bias-corrected NEXGDDP data). Diamonds indicate the value of the location parameter for each distribution. Vertical grey line shows the magnitude of the extreme temperature event on November 18, 2023.

4 Conclusions

The November 2023 heatwave in the city of Rio de Janeiro was a record-breaking event characterized by meteorological conditions largely typical of spring extreme temperature events, but exceptional in their magnitudes. Rising temperatures were associated with positive geopotential height anomalies and corresponding atmospheric subsidence which facilitated clear sky conditions and increased sensible heat flux at the surface. These high pressure anomalies centered over the South Atlantic Subtropical High were likely related to the strong 2023-24 El Niño event. The subsidence near Rio de Janeiro associated with the geopotential height anomalies also suppressed precipitation and facilitated evaporation from the land surface, leading to decreased soil moisture and increased specific humidity. Moisture was available from multiple sources to facilitate these humidity increases, as Rio de Janeiro is a coastal city and downwind of both the Amazon and more local vegetation. SSTs off the coast of Rio de Janeiro were also highly elevated in the days before the heatwave peak, reducing the potential for coastal cooling. Finally, the event was terminated on November 19 due to the evaporative cooling, shading, and mixing associated with the onset of precipitation. The combination of changes in circulation,

land surface feedbacks, and atmosphere-ocean interactions generated the conditions for an exceptionally intense and persistent extreme heat event in the city of Rio de Janeiro.

The risk of extreme heat in austral spring is increasing significantly in Rio de Janeiro. We find that extreme spring temperature events are becoming more frequent and that the extreme heat season is starting earlier and lasting longer than in previous decades. Further, extreme heat of the magnitude on November 18, 2023 may become much more likely by mid- and end-of-century periods. However, the absolute increase in the frequency of similar heatwaves is largely dependent upon our future emissions pathway.

The November 2023 heatwave had devastating impacts, including loss of life. As our climate continues to change and extreme heat in the city of Rio de Janeiro continues to increase in intensity and frequency, we can expect more strain on human health and cascading socioeconomic impacts. This extreme heat event was exceptional not only in its intensity, but also in its persistence. Consecutive extreme heat days have been shown to have nonlinear impacts on human health, in Brazil and in other countries, as they prevent individuals, buildings, and critical electrical equipment from cooling down between heat events (Geirinhas et al., 2020; Baldwin et al., 2019). More broadly, the direct impacts of heatwaves on hospitalizations throughout Brazil have been documented, with the largest effects occurring in long duration events (Zhao et al., 2019). These impacts of heatwaves on mortality are projected to increase, with particular consequences for elderly populations, especially if targeted adaptation measures are not put in place (Diniz et al., 2020). Continuing to improve our understanding of how and when extreme heat occurs is thus essential as our climate continues to change. This is particularly true for locations such as Rio de Janeiro, which historically has not been a hotspot of extreme heat – especially in the shoulder seasons – and thus individuals may not be well acclimated to extreme temperatures then (Periard et al., 2015; Horowitz 2016). The human health impacts of unusually intense events may be exacerbated by the shifting timing of extreme heat, as record-breaking exceptional heat events are now occurring outside of the traditional extreme heat season when individuals may not be prepared to utilize heat mitigation strategies (De Freitas & Grigorieva, 2015). Because Rio de Janeiro is an area of emerging risk for extreme heat, further research on models' ability to capture the historical drivers and timing of heatwaves in this region and evaluations of how these characteristics might shift in the future should be pursued.

540 The meteorological conditions surrounding the extreme heat event analyzed here
541 demonstrate the potential for compound hazards throughout Brazil. The identified circulation
542 pattern that establishes the atmospheric blocking associated with heatwaves in Rio de Janeiro is
543 also likely linked to heavy precipitation events in South Brazil, an extreme case of which
544 occurred in May 2024 in center-north of Rio Grande do Sul, including the metropolitan area of
545 Porto Alegre, displacing hundreds of thousands and killing at least 155 people (Rogerio 2024).
546 The temporal compounding of these extreme temperature and flooding events within Brazil has
547 the potential to strain the country's disaster management systems more than events occurring in
548 isolation. Furthermore, the exceptional spatial area within Brazil that experienced anomalous
549 heat in the November 2023 event, relative to 99th percentile heat events in the city of Rio de
550 Janeiro, underscores the potential for spatially compounding heat that could lead to outsized
551 impacts. Exploring how unprecedented global surface ocean and surface temperatures, along
552 with regional features like the broader heat and drought across much of Brazil, may contribute to
553 extreme heat in the city of Rio de Janeiro will be an important component to improving our
554 understanding of these compound events' drivers, prediction capacity, and potential to change in
555 the future.

556 The evolving meteorological conditions associated with this heatwave were strongly
557 impacted by the lack of precipitation in the first two weeks of November. This is particularly
558 unexpected due to the fact that the active phase of the South American Monsoon System
559 typically begins in late October or early November in this region (Marengo et al., 2012;
560 Liebmann and Mechoso 2011; Raia and Cavalcanti 2008), which is linked to an increase in
561 convective activity in tropical South America in the warm season (Jones and Carvalho 2013).
562 Observational and modeling studies suggest that the South American Monsoon System dry
563 season is lengthening (Arias et al., 2015; Fu et al., 2013) and that the onset of the active phase is
564 delaying (Gomes et al., 2022; Pascale et al., 2019). These trends are projected to continue to
565 some degree in the future with further climate change, particularly in light of ongoing
566 deforestation which contributes to regional drying trends in the Amazon and other areas of Brazil
567 (Boisier et al., 2015; Swann et al., 2015). Given Rio de Janeiro is a city with abundant access to
568 moisture due to its proximity to the coast and vegetation, the increasingly constrained active
569 monsoon phase could lead to increased frequency and intensity of extreme humid heat in the
570 spring season (Ivanovich et al., 2024). These changes could be responsible for the evident

asymmetrical historical increase in heat season length during the spring versus fall as demonstrated here, and extensions of this work should be devoted to an exploration of these potential relationships.

This work highlights the challenge of analyzing the drivers of weather extremes in such a climatically diverse city as Rio de Janeiro and emphasizes the need for future research to explore high resolution comparisons of mechanisms controlling the city's microclimates. Differences between conditions recorded at individual weather stations within the city's boundaries demonstrate the degree to which the dynamics of events in each neighborhood depend on the station's location relative to the coast versus interior (Raymond and Mankin 2019), elevation (Raymond et al., 2022; Pepin et al., 2015), and degree of urbanization (Kruger et al., 2024; Chakraborty et al., 2022; Tan et al., 2010). Higher temporal resolution analysis would also better capture sub-daily processes such as sea breeze and their effect on extreme heat throughout the city. Further, many of these mechanisms influencing the intracity variability of heat stress exposure only focus on the effect of differences in dry bulb temperature. Factoring in the spatial variation in humidity, solar insolation, and windspeed complicate understanding, but are essential for capturing humans' exposure to heat stress conditions. These intracity differences also meaningfully impact compound events with non-heat environmental hazards, such as floods, landslides, droughts, and air pollution, as well as how exposure to these hazards intersects with areas of social vulnerability. Future work should be devoted to investigating the different magnitudes of extreme heat and controlling mechanisms throughout Rio de Janeiro in order to inform targeted extreme heat adaptation plans for individual neighborhoods within the city.

Data Availability: The publicly available datasets used in this analysis are accessible via the following websites: HadISD, <https://www.metoffice.gov.uk/hadobs/hadisd/>; ERA5, <https://cds.climate.copernicus.eu/datasets/reanalysis-era5-single-levels?tab=overview> and <https://cds.climate.copernicus.eu/datasets/reanalysis-era5-pressure-levels?tab=overview>; OISST, <https://www.ncei.noaa.gov/products/optimum-interpolation-sst>; and NEXGDDP, <https://www.nccs.nasa.gov/services/data-collections/land-based-products/nex-gddp-cmip6>. Station data from the Rio Alert System will be uploaded and accessible via a GitHub repository upon manuscript publication.

602 *Code Availability:* All code used for the derivations, calculations, and data visualization will be
603 made publicly available via a GitHub repository upon manuscript publication.

604

605 *Author Contributions:*

606 S.J.C. conceived of the initial project concept. All co-authors contributed to study design, and
607 C.I. performed the analysis. C.I. wrote the initial manuscript draft with the feedback and
608 interpretation of all co-authors. All co-authors read and edited the manuscript.

609

610 *Competing Interests:*

611 The authors declare that they have no conflict of interest.

612

613 *Acknowledgements:*

614 This work was partially supported and funded by Columbia Global at Columbia University,
615 “Simulation of Extreme Weather Events in Brazilian Megacities”, a Climate Hub | Rio Project.
616 Climate Hub | Rio is a knowledge, research, and innovation hub that brings together experts from
617 Brazil, Columbia University, and around the world to advance climate-related knowledge and
618 action in Rio and Brazil. Direct funding for C. Ivanovich and R. Horton was provided by
619 National Oceanic and Atmospheric Administration’s Regional Integrated Sciences and
620 Assessments program, Grant NA15OAR4310147. A. H. Sobel acknowledges support from NSF
621 Grant AGS-1933523. S. J. Camargo is partially supported by the NOAA grant
622 NA23OAR43201600. The authors declare no competing interests.

References

- Alvares, C. A., Stape, J. L., Sentelhas, P. C., & De Moraes Gonçalves, J. L. (2013). Modeling monthly mean air temperature for Brazil. *Theoretical and Applied Climatology*, 113(3–4), 407–427. <https://doi.org/10.1007/s00704-012-0796-6>
- Alvarez, M. S., Vera, C. S., Kiladis, G. N., & Liebmann, B. (2016). Influence of the Madden Julian Oscillation on precipitation and surface air temperature in South America. *Climate Dynamics*, 46(1), 245–262. <https://doi.org/10.1007/s00382-015-2581-6>
- Arias, P. A., Fu, R., Vera, C., & Rojas, M. (2015). A correlated shortening of the North and South American monsoon seasons in the past few decades. *Climate Dynamics*, 45(11), 3183–3203. <https://doi.org/10.1007/s00382-015-2533-1>
- Baldwin, J. W., Dessy, J. B., Vecchi, G. A., & Oppenheimer, M. (2019). Temporally Compound Heat Wave Events and Global Warming: An Emerging Hazard. *Earth's Future*, 7(4), 411–427. <https://doi.org/10.1029/2018EF000989>
- Becker, E., L'Heureux, M., Hu, Z.-Z., & Kumar, A. (2024). ENSO and the tropical Pacific. In “State of the Climate in 2023”. *Bull. Amer. Meteor. Soc.*, 105 (8), S221-S224, <https://doi.org/10.1175/BAMS-D-24-0098.1>
- Bitencourt, Daniel P., Fuentes, M. V., Franke, A. E., Silveira, R. B., & Alves, M. P. A. (2020). The climatology of cold and heat waves in Brazil from 1961 to 2016. *International Journal of Climatology*, 40(4), 2464–2478. <https://doi.org/10.1002/joc.6345>
- Bitencourt, Daniel Pires, Muniz Alves, L., Shibuya, E. K., De Ângelo Da Cunha, I., & Estevam De Souza, J. P. (2021). Climate change impacts on heat stress in Brazil—Past, present, and future implications for occupational heat exposure. *International Journal of Climatology*, 41(S1). <https://doi.org/10.1002/joc.6877>
- Boisier, J. P., Ciais, P., Ducharne, A., & Guimberteau, M. (2015). Projected strengthening of Amazonian dry season by constrained climate model simulations. *Nature Climate Change*, 5(7), 656–660. <https://doi.org/10.1038/nclimate2658>
- Burgess, M. G., Ritchie, J., Shapland, J., & Pielke, R. (2020). IPCC baseline scenarios have over-projected CO2 emissions and economic growth. *Environmental Research Letters*, 16(1), 014016. <https://doi.org/10.1088/1748-9326/abcdd2>
- Cai, W., McPhaden, M. J., Grimm, A. M., Rodrigues, R. R., Taschetto, A. S., Garreaud, R. D., et al., (2020). Climate impacts of the El Niño–Southern Oscillation on South America.

654 Nature Reviews Earth & Environment, 1(4), 215–231. [https://doi.org/10.1038/s43017-](https://doi.org/10.1038/s43017-020-0040-3)
 655 020-0040-3
 656 Castela, R. M., & Barth, J. A. (2006). Upwelling around Cabo Frio, Brazil: The importance of
 657 wind stress curl. *Geophysical Research Letters*, 33(3), 2005GL025182.
 658 <https://doi.org/10.1029/2005GL025182>
 659 Cattiaux, J., Ribes, A., & Cariou, E. (2024). How Extreme Were Daily Global Temperatures in
 660 2023 and Early 2024? *Geophysical Research Letters*, 51(19), e2024GL110531.
 661 <https://doi.org/10.1029/2024GL110531>
 662 Chakraborty, T., Venter, Z. S., Qian, Y., & Lee, X. (2022). Lower Urban Humidity Moderates
 663 Outdoor Heat Stress. *AGU Advances*, 3(5), e2022AV000729.
 664 <https://doi.org/10.1029/2022AV000729>
 665 Cheng, Y.-T., Lung, S.-C. C., & Hwang, J.-S. (2019). New approach to identifying proper
 666 thresholds for a heat warning system using health risk increments. *Environmental*
 667 *Research*, 170, 282–292. <https://doi.org/10.1016/j.envres.2018.12.059>
 668 Cirino, P. H., Féres, J. G., Braga, M. J., & Reis, E. (2015). Assessing the Impacts of ENSO-
 669 related Weather Effects on the Brazilian Agriculture. *Procedia Economics and Finance*,
 670 24, 146–155. [https://doi.org/10.1016/S2212-5671\(15\)00635-8](https://doi.org/10.1016/S2212-5671(15)00635-8)
 671 Coelho, C. A. S., De Souza, D. C., Kubota, P. Y., Cavalcanti, I. F. A., Baker, J. C. A.,
 672 Figueroa, S. N., et al., (2022). Assessing the representation of South American monsoon
 673 features in Brazil and U.K. climate model simulations. *Climate Resilience and*
 674 *Sustainability*, 1(1), e27. <https://doi.org/10.1002/cli2.27>
 675 Coffel, E. D., Horton, R. M., & de Sherbinin, A. (2018). Temperature and humidity based
 676 projections of a rapid rise in global heat stress exposure during the 21st century.
 677 *Environmental Research Letters*, 13(1), 014001. [https://doi.org/10.1088/1748-](https://doi.org/10.1088/1748-9326/aaa00e)
 678 9326/aaa00e
 679 Collazo, S., Barriopedro, D., García-Herrera, R., & Beguería, S. (2025). Extreme heat and
 680 mortality in the state of Rio de Janeiro in November 2023: attribution to climate change
 681 and ENSO. *Natural Hazards and Earth System Sciences*, 25(9), 3221–3238.
 682 <https://doi.org/10.5194/nhess-25-3221-2025>

Formatted: Indent: Left: 0", Hanging: 0.56"

Formatted: Indent: Hanging: 0.5"

683 Collins, J. M., Chaves, R. R., & Marques, V. da S. (2009). Temperature Variability over South
684 America. *Journal of Climate*, 22(22), 5854–5869.
685 <https://doi.org/10.1175/2009JCLI2551.1>

686 Cordero Simões dos Reis, N., Boiaski, N. T., & Ferraz, S. E. T. (2019). Characterization and
687 Spatial Coverage of Heat Waves in Subtropical Brazil. *Atmosphere*, 10(5), 284.
688 <https://doi.org/10.3390/atmos10050284>

689 Correio Braziliense. (2023, November 18). Rio bate recorde de calor do ano neste sábado (18/11)
690 com 42,5°C. Retrieved May 14, 2024, from
691 [https://www.correio braziliense.com.br/brasil/2023/11/6657444-rio-bate-recorde-de-calor-](https://www.correio braziliense.com.br/brasil/2023/11/6657444-rio-bate-recorde-de-calor-do-ano-neste-sabado-18-11-com-425-c.html)
692 [do-ano-neste-sabado-18-11-com-425-c.html](https://www.correio braziliense.com.br/brasil/2023/11/6657444-rio-bate-recorde-de-calor-do-ano-neste-sabado-18-11-com-425-c.html)

693 De Freitas, C., & Grigorieva, E. (2015). Role of Acclimatization in Weather-Related Human
694 Mortality During the Transition Seasons of Autumn and Spring in a Thermally Extreme
695 Mid-Latitude Continental Climate. *International Journal of Environmental Research and*
696 *Public Health*, 12(12), 14974–14987. <https://doi.org/10.3390/ijerph121214962>

697 Dereczynski, C., Silva, W. L., & Marengo, J. (2013). Detection and Projections of Climate
698 Change in Rio de Janeiro, Brazil, 2013. <https://doi.org/10.4236/ajcc.2013.21003>

699 Diniz, F. R., Gonçalves, F. L. T., & Sheridan, S. (2020). Heat Wave and Elderly Mortality:
700 Historical Analysis and Future Projection for Metropolitan Region of São Paulo, Brazil.
701 *Atmosphere*, 11(9), 933. <https://doi.org/10.3390/atmos11090933>

702 Dunn, R. J. H. (2019). HadISD version 3: monthly updates. Hadley Centre Technical Note.

703 Espinoza, J.-C., Jimenez, J. C., Marengo, J. A., Schongart, J., Ronchail, J., Lavado-Casimiro, W.,
704 & Ribeiro, J. V. M. (2024). The new record of drought and warmth in the Amazon in
705 2023 related to regional and global climatic features. *Scientific Reports*, 14(1), 8107.
706 <https://doi.org/10.1038/s41598-024-58782-5>

707 Feron, S., Cordero, R. R., Damiani, A., Llanillo, P. J., Jorquera, J., Sepulveda, E., et al., (2019).
708 Observations and Projections of Heat Waves in South America. *Scientific Reports*, 9(1),
709 8173. <https://doi.org/10.1038/s41598-019-44614-4>

710 Fu, R., Yin, L., Li, W., Arias, P. A., Dickinson, R. E., Huang, L., et al., (2013). Increased dry-
711 season length over southern Amazonia in recent decades and its implication for future
712 climate projection. *Proceedings of the National Academy of Sciences*, 110(45), 18110–
713 18115. <https://doi.org/10.1073/pnas.1302584110>

714 Geirinhas, J. L., Russo, A. C., Libonati, R., Miralles, D. G., Sousa, P. M., Wouters, H., & Trigo,
 715 R. M. (2022). The influence of soil dry-out on the record-breaking hot 2013/2014
 716 summer in Southeast Brazil. *Scientific Reports*, 12(1), 5836.
 717 <https://doi.org/10.1038/s41598-022-09515-z>
 718 Geirinhas, João L., Trigo, R. M., Libonati, R., Coelho, C. A. S., & Palmeira, A. C. (2018).
 719 Climatic and synoptic characterization of heat waves in Brazil. *International Journal of*
 720 *Climatology*, 38(4), 1760–1776. <https://doi.org/10.1002/joc.5294>
 721 Geirinhas, João L., Trigo, R. M., Libonati, R., Castro, L. C. O., Sousa, P. M., Coelho, C. A. S., et
 722 al., (2019). Characterizing the atmospheric conditions during the 2010 heatwave in Rio
 723 de Janeiro marked by excessive mortality rates. *Science of The Total Environment*, 650,
 724 796–808. <https://doi.org/10.1016/j.scitotenv.2018.09.060>
 725 Geirinhas, João L., Russo, A., Libonati, R., Trigo, R. M., Castro, L. C. O., Peres, L. F., et al.,
 726 (2020). Heat-related mortality at the beginning of the twenty-first century in Rio de
 727 Janeiro, Brazil. *International Journal of Biometeorology*, 64(8), 1319–1332.
 728 <https://doi.org/10.1007/s00484-020-01908-x>
 729 Geirinhas, João L., Russo, A., Libonati, R., Sousa, P. M., Miralles, D. G., & Trigo, R. M. (2021).
 730 Recent increasing frequency of compound summer drought and heatwaves in Southeast
 731 Brazil. *Environmental Research Letters*, 16(3), 034036. [https://doi.org/10.1088/1748-](https://doi.org/10.1088/1748-9326/abe0eb)
 732 [9326/abe0eb](https://doi.org/10.1088/1748-9326/abe0eb)
 733 Gomes, G.D., Nunes, A.M.B., Libonati, R., & Ambrizzi, T. (2022). Projections of subcontinental
 734 changes in seasonal precipitation over the two major river basins in South America under
 735 an extreme climate scenario. *Climate Dynamics*, 58, 1147–1169.
 736 <https://doi.org/10.1007/s00382-021-05955-x>
 737 Grimm, A. M. (2019). Madden–Julian Oscillation impacts on South American summer monsoon
 738 season: precipitation anomalies, extreme events, teleconnections, and role in the MJO
 739 cycle. *Climate Dynamics*, 53(1), 907–932. <https://doi.org/10.1007/s00382-019-04622-6>
 740 Hausfather, Z., & Peters, G. P. (2020). Emissions – the ‘business as usual’ story is misleading.
 741 *Nature*, 577(7792), 618–620. <https://doi.org/10.1038/d41586-020-00177-3>
 742 He, Z., Dai, A., & Vuille, M. (2021). The Joint Impacts of Atlantic and Pacific Multidecadal
 743 Variability on South American Precipitation and Temperature. *Journal of Climate*,
 744 34(19), 7959–7981. <https://doi.org/10.1175/JCLI-D-21-0081.1>

745 Hersbach, H., Bell, B., Berrisford, P., Hirahara, S., Horányi, A., Muñoz-Sabater, J., et al., (2020).
 746 The ERA5 global reanalysis. *Quarterly Journal of the Royal Meteorological Society*,
 747 146(730), 1999–2049. <https://doi.org/10.1002/qj.3803>
 748 Horowitz, M. (2016). Epigenetics and cytoprotection with heat acclimation. *Journal of Applied*
 749 *Physiology* (Bethesda, Md.: 1985), 120(6), 702–710.
 750 <https://doi.org/10.1152/japplphysiol.00552.2015>
 751 Huang, B., Liu, C., Banzon, V., Freeman, E., Graham, G., Hankins, B., et al., (2021).
 752 Improvements of the Daily Optimum Interpolation Sea Surface Temperature (DOISST)
 753 Version 2.1. *Journal of Climate*, 34(8), 2923–2939. <https://doi.org/10.1175/JCLI-D-20->
 754 0166.1
 755 Hughs, E., & Jeantet, D. (2023, November 15). It's not yet summer in Brazil, but a dangerous
 756 heat wave is sweeping the country. Retrieved May 14, 2024, from
 757 [https://apnews.com/article/brazil-heat-wave-climate-environment-wildfires-](https://apnews.com/article/brazil-heat-wave-climate-environment-wildfires-1e4714fb2c6566120c13cf4e2b657f7d)
 758 [1e4714fb2c6566120c13cf4e2b657f7d](https://apnews.com/article/brazil-heat-wave-climate-environment-wildfires-1e4714fb2c6566120c13cf4e2b657f7d)
 759 Instituto Brasileiro de Geografia e Estatística. (2022). Demographic Census 2022. Retrieved
 760 from <https://sidra.ibge.gov.br/pesquisa/censo-demografico/demografico-2022/primeiros->
 761 [resultados-populacao-e-domicilios](https://sidra.ibge.gov.br/pesquisa/censo-demografico/demografico-2022/primeiros-)
 762 Ivanovich, C. C., Horton, R. M., Sobel, A. H., & Singh, D. (2024). Subseasonal Variability of
 763 Humid Heat During the South Asian Summer Monsoon. *Geophysical Research Letters*,
 764 51(6), e2023GL107382. <https://doi.org/10.1029/2023GL107382>
 765 Jones, C., & Carvalho, L. M. V. (2013). Climate change in the South American Monsoon
 766 System: Present climate and CMIP5 projections. *Journal of Climate*, 26(17), 6660–6678.
 767 <https://doi.org/10.1175/JCLI-D-12-00412.1>
 768 Jornal Nacional. (2023, November 18). Taylor Swift: segundo show é adiado, por causa do calor
 769 extremo no Rio. Retrieved April 16, 2024, from <https://g1.globo.com/jornal->
 770 [nacional/noticia/2023/11/18/taylor-swift-show-e-adiado-apos-morte-de-fa.ghml](https://g1.globo.com/jornal-)
 771 Krüger, E., Gobo, J. P. A., Tejas, G. T., da Silva de Souza, R. M., Neto, J. B. F., Pereira, G., et
 772 al., (2024). The impact of urbanization on heat stress in Brazil: A multi-city study. *Urban*
 773 *Climate*, 53, 101827. <https://doi.org/10.1016/j.uclim.2024.101827>

774 Lanzante, J. R., Dixon, K. W., Nath, M. J., Whitlock, C. E., & Adams-Smith, D. (2018). Some
 775 Pitfalls in Statistical Downscaling of Future Climate. *Bulletin of the American*
 776 *Meteorological Society*, 99(4), 791–803. <https://doi.org/10.1175/BAMS-D-17-0046.1>
 777 Latinović, D., Chou, S. C., Rančić, M., Medeiros, G. S., & Lyra, A. D. A. (2019).
 778 Seasonal climate and the onset of the rainy season in western-central Brazil simulated by
 779 Global Eta Framework model. *International Journal of Climatology*, 39(3), 1429–1445.
 780 <https://doi.org/10.1002/joc.5892>
 781 Lemus-Canovas, M., Insua-Costa, D., Trigo, R. M., & Miralles, D. G. (2024). Record-shattering
 782 2023 Spring heatwave in western Mediterranean amplified by long-term drought. *Npj*
 783 *Climate and Atmospheric Science*, 7(1), 1–8. [https://doi.org/10.1038/s41612-024-00569-](https://doi.org/10.1038/s41612-024-00569-6)
 784 6
 785 Libonati, R., Geirinhas, J. L., Silva, P. S., Monteiro Dos Santos, D., Rodrigues, J. A., Russo, A.,
 786 et al., (2022). Drought–heatwave nexus in Brazil and related impacts on health and fires:
 787 A comprehensive review. *Annals of the New York Academy of Sciences*, 1517(1), 44–
 788 62. <https://doi.org/10.1111/nyas.14887>
 789 Liebmann, B., & Mechoso, C. R. (2011). THE SOUTH AMERICAN MONSOON SYSTEM. In
 790 C.-P. Chang, Y. Ding, N.-C. Lau, R. H. Johnson, B. Wang, & T. Yasunari, *World*
 791 *Scientific Series on Asia-Pacific Weather and Climate* (2nd ed., Vol. 5, pp. 137–157).
 792 WORLD SCIENTIFIC. https://doi.org/10.1142/9789814343411_0009
 793 Lyra, G. B., Correia, T. P., de Oliveira-Júnior, J. F., & Zeri, M. (2018). Evaluation of methods of
 794 spatial interpolation for monthly rainfall data over the state of Rio de Janeiro, Brazil.
 795 *Theoretical and Applied Climatology*, 134(3), 955–965. [https://doi.org/10.1007/s00704-](https://doi.org/10.1007/s00704-017-2322-3)
 796 017-2322-3
 797 Marengo, J. A., Liebmann, B., Grimm, A. M., Misra, V., Silva Dias, P. L., Cavalcanti, I. F. A., et
 798 al., (2012). Recent developments on the South American monsoon system. *International*
 799 *Journal of Climatology*, 32(1), 1–21. <https://doi.org/10.1002/joc.2254>
 800 Marengo, Jose A., Soares, W. R., Saulo, C., & Nicolini, M. (2004). Climatology of the Low-
 801 Level Jet East of the Andes as Derived from the NCEP–NCAR Reanalyses:
 802 Characteristics and Temporal Variability. *Journal of Climate*, 17(12), 2261–2280.
 803 [https://doi.org/10.1175/1520-0442\(2004\)017<2261:COTLJE>2.0.CO;2](https://doi.org/10.1175/1520-0442(2004)017<2261:COTLJE>2.0.CO;2)

804 Montini, T. L., Jones, C., & Carvalho, L. M. V. (2019). The South American Low-Level Jet: A
 805 New Climatology, Variability, and Changes. *Journal of Geophysical Research:*
 806 *Atmospheres*, 124(3), 1200–1218. <https://doi.org/10.1029/2018JD029634>
 807 Mora, C., Dousset, B., Caldwell, I. R., Powell, F. E., Geronimo, R. C., Bielecki, C. R., et
 808 al., (2017). Global risk of deadly heat. *Nature Climate Change*, 7(7), 501–506.
 809 <https://doi.org/10.1038/nclimate3322>
 810 Nahlik, M. J., Chester, M. V., Pincetl, S. S., Eisenman, D., Sivaraman, D., & English, P. (2017).
 811 Building Thermal Performance, Extreme Heat, and Climate Change. *Journal of*
 812 *Infrastructure Systems*, 23(3), 04016043. [https://doi.org/10.1061/\(asce\)is.1943-](https://doi.org/10.1061/(asce)is.1943-)
 813 [555x.0000349](https://doi.org/10.1061/(asce)is.1943-555x.0000349)
 814 NASA JPL. (2024, January 23). El Niño 2023 | El Niño/La Niña Watch & PDO. Retrieved May
 815 14, 2024, from [https://sealevel.jpl.nasa.gov/data/el-nino-la-nina-watch-and-pdo/el-nino-](https://sealevel.jpl.nasa.gov/data/el-nino-la-nina-watch-and-pdo/el-nino-2023)
 816 [2023](https://sealevel.jpl.nasa.gov/data/el-nino-la-nina-watch-and-pdo/el-nino-2023)
 817 Nguyen, B. (2023, December 27). Brazilian Taylor Swift Fan Died Of Heat Exhaustion At Rio
 818 Concert. Retrieved April 16, 2024, from
 819 [https://www.forbes.com/sites/britneynguyen/2023/12/27/brazilian-taylor-swift-fan-died-](https://www.forbes.com/sites/britneynguyen/2023/12/27/brazilian-taylor-swift-fan-died-of-heat-exhaustion-at-rio-concert/)
 820 [of-heat-exhaustion-at-rio-concert/](https://www.forbes.com/sites/britneynguyen/2023/12/27/brazilian-taylor-swift-fan-died-of-heat-exhaustion-at-rio-concert/)
 821 Palma, E. D., & Matano, R. P. (2009). Disentangling the upwelling mechanisms of the South
 822 Brazil Bight. *Continental Shelf Research*, 29(11), 1525–1534.
 823 <https://doi.org/10.1016/j.csr.2009.04.002>
 824 [Pampuch, L. A., Bueno, P. G., Reboita, M. S., Tomaziello, A. C. N., Nunes, A. M. P., Cardoso,](#)
 825 [A. A., et al. \(2025\). Brazil climate highlights 2023. *Annals of the New York Academy of*](#)
 826 [Sciences, 1549\(1\), 120–138. <https://doi.org/10.1111/nyas.15394>](#)
 827 Pascale, S., Carvalho, L. M. V., Adams, D. K., Castro, C. L., & Cavalcanti, I. F. A. (2019).
 828 Current and Future Variations of the Monsoons of the Americas in a Warming Climate.
 829 *Current Climate Change Reports*, 5(3), 125–144. <https://doi.org/10.1007/s40641-019->
 830 [00135-w](https://doi.org/10.1007/s40641-019-00135-w)
 831 Pepin, N., Bradley, R. S., Diaz, H. F., Baraer, M., Caceres, E. B., Forsythe, N., et al., (2015).
 832 Elevation-dependent warming in mountain regions of the world. *Nature Climate Change*,
 833 5(5), 424–430. <https://doi.org/10.1038/nclimate2563>

834 Périard, J. D., Racinais, S., & Sawka, M. N. (2015). Adaptations and mechanisms of human heat
835 acclimation: Applications for competitive athletes and sports. *Scandinavian Journal of*
836 *Medicine & Science in Sports*, 25 Suppl 1, 20–38. <https://doi.org/10.1111/sms.12408>

837 Powis, C. M., Byrne, D., Zobel, Z., Gassert, K. N., Lute, A. C., & Schwalm, C. R. (2023).
838 Observational and model evidence together support wide-spread exposure to
839 noncompensable heat under continued global warming. *Science Advances*, 9(36),
840 eadg9297. <https://doi.org/10.1126/sciadv.adg9297>

841 [Perkins-Kirkpatrick, S., Barriopedro, D., Jha, R., Wang, L., Mondal, A., Libonati, R., &](#)
842 [Kornhuber, K. \(2024\). Extreme terrestrial heat in 2023. *Nature Reviews Earth &*](#)
843 [Environment](#), 5(4), 244–246. <https://doi.org/10.1038/s43017-024-00536-y>

844 Perkins, S. E., Pitman, A. J., Holbrook, N. J., & McAneney, J. (2007). Evaluation of the AR4
845 Climate Models' Simulated Daily Maximum Temperature, Minimum Temperature, and
846 Precipitation over Australia Using Probability Density Functions. *Journal of Climate*,
847 20(17), 4356–4376. <https://doi.org/10.1175/JCLI4253.1>

848 Raia, A., & Cavalcanti, I. F. A. (2008). The Life Cycle of the South American Monsoon System.
849 *Journal of Climate*, 21(23), 6227–6246. <https://doi.org/10.1175/2008JCLI2249.1>

850 Raymond, C., & Mankin, J. S. (2019). Assessing present and future coastal moderation of
851 extreme heat in the Eastern United States. *Environmental Research Letters*, 14(11),
852 114002. <https://doi.org/10.1088/1748-9326/ab495d>

853 Raymond, C., Matthews, T., & Horton, R. M. (2020). The emergence of heat and humidity too
854 severe for human tolerance. *Science Advances*, 6(19), eaaw1838.
855 <https://doi.org/10.1126/sciadv.aaw1838>

856 Raymond, C., Waliser, D., Guan, B., Lee, H., Loikith, P., Massoud, E., et al., (2022). Regional
857 and Elevational Patterns of Extreme Heat Stress Change in the US. *Environmental*
858 *Research Letters*. <https://doi.org/10.1088/1748-9326/ac7343>

859 Regoto, P., Dereczynski, C., Chou, S. C., & Bazzanella, A. C. (2021). Observed changes in air
860 temperature and precipitation extremes over Brazil. *International Journal of Climatology*,
861 41(11), 5125–5142. <https://doi.org/10.1002/joc.7119>

862 Rehbein, A., & Ambrizzi, T. (2023). ENSO teleconnections pathways in South America. *Climate*
863 *Dynamics*, 61(3), 1277–1292. <https://doi.org/10.1007/s00382-022-06624-3>

Formatted: Don't add space between paragraphs of the same style

864 Ritchie, J., & Dowlatabadi, H. (2017). Why do climate change scenarios return to coal? *Energy*,
865 140, 1276–1291. <https://doi.org/10.1016/j.energy.2017.08.083>

866 Rogero, T. (2024, May 19). Brazil counts cost of worst-ever floods with little hope of waters
867 receding soon. *The Guardian*. Retrieved from
868 <https://www.theguardian.com/world/article/2024/may/19/brazil-floods-toll>

869 Rogers, C. D. W., Ting, M., Li, C., Kornhuber, K., Coffel, E. D., Horton, R. M., et al., (2021).
870 Recent Increases in Exposure to Extreme Humid-Heat Events Disproportionately Affect
871 Populated Regions. *Geophysical Research Letters*, 48(19).
872 <https://doi.org/10.1029/2021GL094183>

873 Shimizu, M. H., & Ambrizzi, T. (2016). MJO influence on ENSO effects in precipitation and
874 temperature over South America. *Theoretical and Applied Climatology*, 124(1), 291–301.
875 <https://doi.org/10.1007/s00704-015-1421-2>

876 Shreevastava, A., Raymond, C., & Hulley, G. C. (2023). Contrasting Intraurban Signatures of
877 Humid and Dry Heatwaves over Southern California. *Journal of Applied Meteorology*
878 and *Climatology*, 62(6), 709–720. <https://doi.org/10.1175/JAMC-D-22-0149.1>

879 Sistema Alerta Rio da Prefeitura do Rio de Janeiro. (2024). Meteorological Data. Retrieved from
880 <https://alertario.rio.rj.gov.br/download/dados-meteorologicos/>

881 Sistema IBGE de Recuperação Automática - SIDRA. (n.d.). Retrieved April 21, 2024, from
882 <https://sidra.ibge.gov.br/pesquisa/censo-demografico/demografico-2022/primeiros->
883 [resultados-populacao-e-domicilios](https://sidra.ibge.gov.br/pesquisa/censo-demografico/demografico-2022/primeiros-resultados-populacao-e-domicilios)

884 Son, J.-Y., Gouveia, N., Bravo, M. A., de Freitas, C. U., & Bell, M. L. (2016). The impact of
885 temperature on mortality in a subtropical city: effects of cold, heat, and heat waves in São
886 Paulo, Brazil. *International Journal of Biometeorology*, 60(1), 113–121.
887 <https://doi.org/10.1007/s00484-015-1009-7>

888 Stefanello, M., Ewerling da Rosa, C., Bresciani, C., Cordero Simões dos Reis, N., Stefanello
889 Facco, D., Teleginski Ferraz, S. E., et al., (2022). Spatial–temporal analysis of a summer
890 heat wave associated with downslope flows in southern Brazil: implications in the
891 atmospheric boundary layer. *Atmosphere* 14(1). 64.
892 <https://doi.org/10.3390/atmos14010064>

893 Swann, A. L. S., Longo, M., Knox, R. G., Lee, E., & Moorcroft, P. R. (2015). Future
894 deforestation in the Amazon and consequences for South American climate. *Agricultural*

895 and Forest Meteorology, 214–215, 12–24.
896 <https://doi.org/10.1016/j.agrformet.2015.07.006>
897 Tan, J., Zheng, Y., Tang, X., Guo, C., Li, L., Song, G., et al., (2010). The urban heat island and
898 its impact on heat waves and human health in Shanghai. *International Journal of*
899 *Biometeorology*, 54(1), 75–84. <https://doi.org/10.1007/s00484-009-0256-x>
900 Thrasher, B., Wang, W., Michaelis, A., Melton, F., Lee, T., & Nemani, R. (2022). NASA Global
901 Daily Downscaled Projections, CMIP6. *Scientific Data*, 9(1), 262.
902 <https://doi.org/10.1038/s41597-022-01393-4>
903 United Nations Department of Economic and Social Affairs Population Division. (2022).
904 Population of Urban Agglomerations with 300,000 Inhabitants or More in 2018, by
905 country, 1950-2035 (thousands). Retrieved from
906 <https://population.un.org/wup/Download/>
907 US EPA, O. (2021, February 4). Climate Change Indicators: Heat Waves [Reports and
908 Assessments]. Retrieved April 23, 2024, from [https://www.epa.gov/climate-](https://www.epa.gov/climate-indicators/climate-change-indicators-heat-waves)
909 [indicators/climate-change-indicators-heat-waves](https://www.epa.gov/climate-indicators/climate-change-indicators-heat-waves)
910 Vecellio, D. J., Wolf, S. T., Cottle, R. M., & Kenney, W. L. (2022). Evaluating the 35°C wet-
911 bulb temperature adaptability threshold for young, healthy subjects (PSU HEAT Project).
912 *Journal of Applied Physiology*, 132(2), 340–345.
913 <https://doi.org/10.1152/japplphysiol.00738.2021>
914 Vera, C., Baez, J., Douglas, M., Emmanuel, C. B., Marengo, J., Meitin, J., et al., (2006). The
915 South American Low-Level Jet Experiment. *Bulletin of the American Meteorological*
916 *Society*, 87(1), 63–78. <https://doi.org/10.1175/BAMS-87-1-63>
917 Wilby, R. L., Kasei, R., Gough, K. V., Amankwaa, E. F., Abarike, M., Anderson, N. J., et al.,
918 (2021). Monitoring and moderating extreme indoor temperatures in low-income urban
919 communities. *Environmental Research Letters*, 16(2), 024033.
920 <https://doi.org/10.1088/1748-9326/abdbf2>
921 You, Y., Ting, M., & Biasutti, M. (2024). Climate warming contributes to the record-shattering
922 2022 Pakistan rainfall. *Npj Climate and Atmospheric Science*, 7(1), 1–8.
923 <https://doi.org/10.1038/s41612-024-00630-4>
924 Zhao, Q., Li, S., Coelho, M. S. Z. S., Saldiva, P. H. N., Hu, K., Huxley, R. R., et al., (2019). The
925 association between heatwaves and risk of hospitalization in Brazil: A nationwide time

926 series study between 2000 and 2015. PLOS Medicine, 16(2), e1002753.
927 <https://doi.org/10.1371/journal.pmed.1002753>